ELSEVIER

Chemical Engineering Journal 115 (2005) 85–92

Chemical Engineering Journal

www.elsevier.com/locate/cej

Experimental and CFD investigation on mixing by a jet in a semi-industrial stirred tank

Masoud Rahimi *, Arsalan Parvareh

Chemical Engineering Department, Baghe Abrisham, Taghe Bostan, Faculty of Engineering, Razi University, Kermanshah 67149, Iran

Received 15 April 2005; received in revised form 14 September 2005; accepted 27 September 2005

Abstract

This paper reports the results of a study on the flow generated and mixing time in a semi-industrial tank equipped with a side entry jet mixer. For this purpose, a three dimensional modeling is carried out using an in-house Computational Fluid Dynamics (CFD) code. In this study, the theoretical mixing curves predicted by the CFD were validated by experiments. The experimental mixing curves were obtained by monitoring of the homogenization progress of the dark blue Nigrosine solution inside the tank. A photometer equipped with an online detector was used for this purpose. The experiments were carried out for 0°, 22.5° and 45° jet angle setups. The results showed that the mixing time in the 45° jet layout is lower than other setups.

The CFD code with the ability of simultaneous solving of the continuity, the Reynolds-averaged Navier–Stokes (RANS) equations and employing various types of turbulence models was used. The effect of the mesh size on the predicted results was investigated and the theoretical results obtained from various mesh sizes configuration were compared with the experiments. The results showed that the number of meshes is quite effective on the obtained theoretical results in a way that the predicted results for the largest mesh size were far away from the experiments. In addition, the two equation k–ε family models including: standard, RNG and realizable models were introduced to the code and the effect of these models on the predicted results was investigated. The results show that there are considerable differences between the predicted mixing progress using the three versions of the k–ε family models. The RNG k–ε model shows more convincing results in comparison with the other models.

Keywords: Mixing; CFD; Stirred tanks; Jet; Turbulence model

1. Introduction

Mixing in stirred tanks is a common practice in many chemical, oil and petrochemical industries. Stirred tanks are widely used in the process industries to carry out many different operations including, blending of miscible liquids into a single liquid phase, suspension of solids, heat and mass transfer promotion, chemical reaction, etc.

Mixing by impellers and jets are two known methods for fluid homogenization in the liquid phase. The jet mixers are cheap and are easily installed relative to the impeller mixers. A jet needs just a pump for fluid circulating, a cheap nozzle and some simple piping works. In the jet mixing, a part of the liquid inside the tank is drawn through a pump and returned into the tank. Therefore, similar to the mixing by an impeller, a circulating pattern is maintained in the tank by a jet which causes liquid homogenization.

Numerous research studies have been undertaken to investigate the jet mixing using various approaches of numerical modeling. A part of these studies tries to propose empirical equations which relates the mixing time as an important criterion in mixing to the operation conditions and geometries. In addition, many studies focused on the modeling of the fluid flow hydrodynamic in the laboratory scales and validating the predicted results using various experimental methods. This was achieved due to the development of advanced computer modeling techniques such as the CFD.

One of the earliest studies on jet mixing was carried out by Fossett [1]. He experimentally investigated the use of an inclined side entry jet to mix large scale storage tanks. The following

* Corresponding author.
E-mail address: masoudrahimi@yahoo.com (M. Rahimi).

1385-8947/$ – see front matter © 2005 Elsevier B.V. All rights reserved.
doi:10.1016/j.cej.2005.09.021

Nomenclature

C_1, C_2, C_μ constants of the k–ε model
E_{ij} linear deformation rate, (s^{-1})
G dissipation function, (pa s^{-1})
k turbulent kinetic energy (J kg^{-1})
S source term
U velocity vector (m s^{-1})
u, v, w, u_i, u_j mean velocity components (m s^{-1})
u', v', w', u'_i, u'_j turbulent fluctuating velocity component (m s^{-1})
x_i, x_j Cartesian coordinate (m)

Greek symbols
ε dissipation rate of k (W kg^{-1})
Φ, φ' mean and turbulent fluctuating values of scalar property
Γ scalar diffusion coefficient
μ, μ_T, μ_{eff} laminar, turbulent and effective viscosities (Pa s)
v_T, v_{eff} turbulent and effective kinematics viscosity
ρ density (kg m^{-3})
σ_k, σ_ε turbulent Prandtl numbers for k–ε

correlation was proposed for determining the mixing time (T_m) in the tank:

$$T_m = \frac{9D^2}{Vd} \tag{1}$$

in which D is the tank diameter, d the jet diameter and V is the jet velocity. This study extended by Fox and Gex [2], who proposed a modified version of Eq. (1). They monitored the solution pH as a criterion for the mixing progress. Lane and Rice [3] studied mixing by a vertical jet mixer in a round bottom vessel. They observed that homogenization time depends on the jet Reynolds number in the laminar regime, while in the turbulent cases the jet Reynolds number is not too important. The effect of the injection position on the mixing time, were studied by Yianneskis [4]. He reported that the position of the probe and tracer injection point do not have a significant effect on the final homogenization time.

The CFD modeling of mixing in process industries has attracted a lot of attention since 1990. This technique was developed due to the availability of advance measurement techniques for validating the theoretical results. Unger et al. [5] characterized the laminar viscous flow in an impinging jet contactor using the CFD modeling and Particle Image Velocimetry (PIV) measurement. They found that mixing will improve substantially if the geometry be asymmetric. Following on this study, Unger and Muzzio [6] used the Laser-Induced Fluorescence (LIF) technique in order to quantitatively compare the mixing performance between the two impinging jet geometries.

Brooker [7] studied the performance of jet mixing using the CFD. In this work, an error of 15% in the mixing time was reported. This work focused on the overall mixing time instead of the homogenization progress trend. The flow pattern and the mixing time in a jet mixed tank equipped with various types of jet were predicted by Ranade [8]. He used the standard k–ε model in his CFD modeling. A non convincing validation of the predicted results with the experiment was reported. Jayanti [9] studied the hydrodynamics of jet mixing using various jet configurations in a cylindrical vessel. He tried to find a way to reduce the mixing time by eliminating the dead zones in the vessel. Patwardhan [10] compared the CFD prediction and the experimental mixing results of sodium chloride solution in a 98 l tank. He concluded that the CFD modeling is quite satisfactory for predicting mixing time but it is poor in predicting the homogenization progress. The effect of the jet angle and the number of jets on the mixing time were studied by Zughbi and Rakib [11]. Their three dimensional modeling showed that the angle of jet injection is the most important parameter for determining the mixing time. In a recent research by Feng et al. [12] the velocity and concentration fields in a confined planar-jet reactor measured using PIV and LIF techniques. The CFD prediction were validated by the obtained experimental results and a good agreement was reported by authors.

2. Theory

The CFD modeling involves the numerical solution of the conservation equations in the laminar and turbulent fluid flow regimes. Therefore, the theoretical predictions were obtained by simultaneous solution of the continuity and the Reynolds-averaged Navier–Stokes (RANS) equations.

The crucial difference between the modeling of laminar and turbulent flows is the appearance of eddying motions of a wide range of length scales in the turbulent flows. The random nature of a turbulent flow precludes computations based on a complete description of the motion of all the fluid particles. In general, it is most attractive to characterize the turbulent flow by the mean values of flow properties and the statistical properties of their fluctuations. Introducing the time-averaged properties for the flow (mean velocities, mean pressures and mean stresses) to the time dependent Navier–Stokes equations, lead to time-averaged Navier–Stokes equations as follows (Versteeg and Malalasekera [13]):

Continuity equation:

$$\frac{\partial \rho}{\partial t} + \mathrm{div}(\rho \mathbf{U}) = 0 \tag{2}$$

Momentum equations:

$$\frac{\partial(\rho u)}{\partial t} + \mathrm{div}(\rho u \mathbf{U}) = -\frac{\partial p}{\partial x} + \mathrm{div}(\mu\, \mathrm{grad}\, u) + \left[-\frac{\partial(\rho \overline{u'^2})}{\partial x} - \frac{\partial(\rho \overline{u'v'})}{\partial y} - \frac{\partial(\rho \overline{u'w'})}{\partial z} \right] + S_{Mx} \tag{3}$$

$$\frac{\partial(\rho v)}{\partial t} + \mathrm{div}(\rho v \mathbf{U}) = -\frac{\partial p}{\partial y} + \mathrm{div}(\mu\ \mathrm{grad}\ v) + \left[-\frac{\partial(\rho\overline{u'v'})}{\partial x} - \frac{\partial(\rho\overline{v'^2})}{\partial y} - \frac{\partial(\rho\overline{v'w'})}{\partial z}\right] + S_{\mathrm{My}} \quad (4)$$

$$\frac{\partial(\rho w)}{\partial t} + \mathrm{div}(\rho w \mathbf{U}) = -\frac{\partial p}{\partial z} + \mathrm{div}(\mu\ \mathrm{grad}\ w) + \left[-\frac{\partial(\rho\overline{u'w'})}{\partial x} - \frac{\partial(\rho\overline{v'w'})}{\partial y} - \frac{\partial(\rho\overline{w'^2})}{\partial z}\right] + S_{\mathrm{Mz}} \quad (5)$$

and the transport equation for scalar property Φ is:

$$\frac{\partial \Phi}{\partial t} + \mathrm{div}(\Phi \mathbf{U}) = \mathrm{div}(\Gamma^*_\Phi\ \mathrm{grad}\ \Phi) + \left[-\frac{\partial\overline{u'\varphi'}}{\partial x} - \frac{\partial\overline{u'\varphi'}}{\partial y} - \frac{\partial\overline{u'\varphi'}}{\partial z}\right] + S_\Phi \quad (6)$$

which in general notation:

$$-\rho\overline{u'_i u'_j} = \tau_{ij} = \mu_{\mathrm{T}}\left(\frac{\partial u_i}{\partial x_j} + \frac{\partial u_j}{\partial x_i}\right) \quad (7)$$

$$\mu_{\mathrm{T}} = \rho C_\mu \frac{k^2}{\varepsilon} \quad (8)$$

A turbulence model is a computational procedure to calculate μ_{T}. The Reynolds stress terms, u'_i and u'_j, can be defined on the basis of time-averaged velocity component.

In the present work, a three dimensional fluid hydrodynamics modeling was performed using an in-house CFD code. In order to involve the effect of the turbulence model on the predicted results three models were employed. The models were selected from the two equations k–ε family model including: the standard, RNG and realizable. The two-equation k–ε model consists of an equation for the turbulent kinetic energy, k, and the other for the energy dissipation rate, ε, as are described in the following equations:

$$\frac{\partial(\rho k)}{\partial t} + \frac{\partial}{\partial x_i}(\rho u_i k) = \frac{\partial}{\partial x_i}\left(\rho\frac{v_{\mathrm{eff}}}{\sigma_k}\frac{\partial k}{\partial x_i}\right) + \rho(P_k - \varepsilon) \quad (9)$$

$$\frac{\partial(\rho\varepsilon)}{\partial t} + \frac{\partial}{\partial x_i}(\rho u_i \varepsilon) = \frac{\partial}{\partial x_i}\left(\rho\frac{v_{\mathrm{eff}}}{\sigma_\varepsilon}\frac{\partial \varepsilon}{\partial x_i}\right) + S_\varepsilon \quad (10)$$

where

$$\nu_{\mathrm{eff}} = \frac{\mu_{\mathrm{eff}}}{\rho} \quad \text{and} \quad \mu_{\mathrm{eff}} = \mu + \mu_{\mathrm{T}} \quad (11)$$

As can be seen in the Eqs. (9) and (10), the relations are the same as the general transport equations, with the source terms, S_ε, defined in different ways for each model. Table 1 illustrates the S_ε relations for the k–ε family models. The relation for P_k is as follows:

$$P_k = v_t\left(\frac{\partial u_i}{\partial x_j} + \frac{\partial u_j}{\partial x_i}\right)\frac{\partial u_i}{\partial x_j} \quad (12)$$

The standard k–ε model is a semi-empirical model based on transport equations for the turbulent kinetic energy (k) and its dissipation rate (ε). As the strengths and weaknesses of the standard k–ε model have become known, improvements have been made to the model to improve its performance by the RNG and realizable models.

In the RNG k–ε model, the effect of small-scale turbulence is represented by means of a random forcing function in the Navier–Stokes equations. The RNG procedure systematically removes the small scales of motion from the governing equations by expressing their effects in terms of larger-scale motion and a modified viscosity. The realizable k–ε model is a relatively recent development and contains a new formulation for the turbulent viscosity and a new transport equation for the dissipation rate, ε. It has been derived from an exact equation for the transport of the mean-square vorticity fluctuation. Both the realizable and RNG k–ε models have shown substantial improvements over the standard k–ε model where the flow features include strong streamline curvature, vortices and rotation.

Table 1
The S_ε definition in k–ε family turbulence models

Model	S_ε	Parameters
Standard (Launder and Spalding [14])	$\rho\left(C_{1,S}\frac{\varepsilon}{k}P_k - C_{2,S}\frac{\varepsilon}{k}\varepsilon\right)$	$C_{\mu,S} = 0.09$; $C_{1,S} = 1.44$; $C_{2,S} = 1.92$; $\sigma_{k,S} = 1$; $\sigma_{\varepsilon,S} = 1.314$
RNG (Yakhot and Orszag [15])	$\rho\left(C_{1,\mathrm{RNG}}\frac{\varepsilon}{k}P_k - \alpha\frac{\varepsilon}{k}\varepsilon - C_{2,\mathrm{RNG}}\frac{\varepsilon}{k}\varepsilon\right)$	$\alpha = C_\mu\eta^3\frac{1-\eta/\eta_0}{1+\beta\eta^3}$; $C_{\mu,\mathrm{RNG}} = 0.0845$; $C_{1,\mathrm{RNG}} = 1.42$; $C_{2,\mathrm{RNG}} = 1.68$; $\sigma_{k,\mathrm{RNG}} = \sigma_{\varepsilon,\mathrm{RNG}} = 0.719$; $\eta_0 = 4.8$; $\beta = 0.012$; $\eta = E\frac{k}{\varepsilon}$; $E^2 = 2E_{ij}E_{ij}$; $E_{ij} = 0.5\left(\frac{\partial u_i}{\partial x_j} + \frac{\partial u_j}{\partial x_i}\right)$
Realizable (Shih et al. [16])	$\rho\left(C_{1,\mathrm{Re}}E\varepsilon - C_{2,\mathrm{Re}}\frac{\varepsilon^2}{k+\sqrt{v\varepsilon}}\right)$	$C_{1,Re} = \max\left[0.43;\ \frac{\eta}{\eta+5}\right]$; $C_{\mu,\mathrm{Re}} = 0.09$; $C_{2,\mathrm{Re}} = 1.9$; $\sigma_{k,\mathrm{Re}} = 1$; $\sigma_{\varepsilon,\mathrm{Re}} = 1.2$; $\eta = E\frac{k}{\varepsilon}$; $E^2 = 2E_{ij}E_{ij}$; $E_{ij} = 0.5\left(\frac{\partial u_i}{\partial x_j} + \frac{\partial u_j}{\partial x_i}\right)$

Fig. 1. The floating roof stirred tank and its components.

3. Experimental work

In the present research, the mixing in a semi-industrial 130 l floating roof tank with a diameter of 90 cm and a height of 20 cm was studied. The height to diameter ratio of the tank is quite similar to the large scale floating roof crude oil storage tanks [17,18]. In real floating roof tank, the roof is heavy and is exactly placed upon the fluid to prevent volatile material accumulation in the space between the liquid surface and the roof. This is very important from the safety point of view. In the experiment, a heavy object was put upon the roof similar to the real tanks.

In order to study the homogenization progress inside the tank, the Nigrosine dye solution was used as a tracer in the experiments. A 65 cm^3 of this solution was injected during 4 s via an automatic injector system. The tracer spreading was detected by a photometer made by Metrohm Company which equipped it by an online probe. The photometer probe is sensitive to the opacity of the fluid placed between the light emitter and sensor. Fig. 1 illustrates the rig and the jet which was installed inside the tank. The probe and its position as well as the tracer injection position are shown in the figure.

As a first step of the experimental work, the tank was equipped with a jet with a diameter of 0.5 cm. The angle of the jet with the horizon was adjusted to be zero degree. Water with a linear velocity of 4.25 m/s was diverted into the tank via the jet. The discharge pipe was placed in the opposite side of the jet at the same elevation. In the next two sets of the experiments, the 0° nozzle was replaced by the 22.5° and 45° ones.

The obtained mixing curves for the three experimental setups are shown in Fig. 2. Each run was carried out three times and the presented mixing curves are averaged ones. The difference in the value of the overall mixing time was less than 5%. The figure shows that the smallest mixing time was obtained in the 45° jet angle setup. The overall mixing time in the 22.5° jet is almost doubles and the 0° jet has the slowest tracer spreading process.

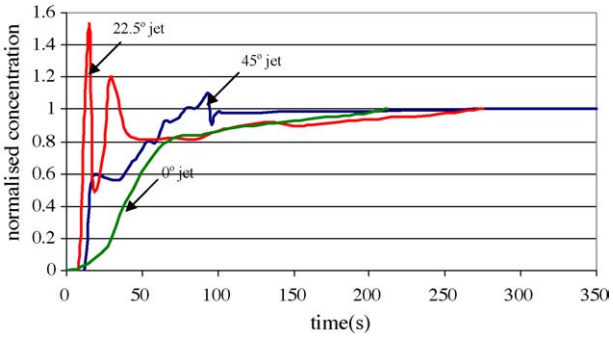

Fig. 2. The experimental mixing curves for various jet setups.

4. CFD modeling

In the present research, an in-house finite volume CFD code with the ability to model the mixing in three dimensions was used. The tank was assumed to be the fixed roof regarding to experiment setup as explained before. The tank was meshed into various numbers of the tetrahedral cell. A part of the meshed tank and the modeled jet inside the tank is illustrated in Fig. 3. The SIMPLE pressure–velocity coupling algorithm, the standard pressure, the first order upwind discretization scheme for momentum, turbulent kinetic energy and dissipation energy were employed in the modeling. In addition, the 0.001 convergence criterion was chosen in the modeling.

In this study, three jet setups with angles of 0°, 22.5° and 45° respect to the horizon were modeled. Similar to the experiments a velocity of 4.25 m/s was introduced as the jet outflow velocity for the whole cross sectional area of the jet. In the first part of the modeling, the steady state solution was obtained and the three dimensional velocity profiles and the other fluid flow hydrodynamics parameters were found.

After the fluid flow pattern was established, the unsteady run was carried out as the tracer was injected. The volumetric rate of the tracer injection was calculated from the amount of the tracer injected in the experiment and a linear injection velocity of

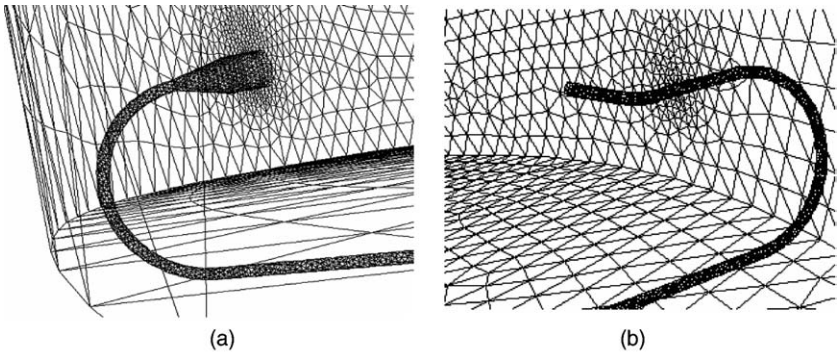

Fig. 3. The meshed tank at the nozzle and discharge sections.

1.3 m/s was obtained. In the model, this velocity was introduced to the zones placed at the injector position during the injection. In addition, during this period these zones diverting the tracer inside the tank. The obtained tracer concentration was related to the photometer reading number according to the initial prepared calibrated curve in the experiment.

5. Results and discussion

Fig. 4 shows examples of the predicted flow fields in an arbitrary vertical slice going through the jets and the discharge pipes in the three jet layouts using the RNG version of the k–ε model. The equal size velocity vectors are used in order to illustrate the fluid flow pattern inside the tank.

As can be seen in the figure, the generated flow hit the tank roof in 45° jet setup at almost one-third of the tank radius from the jet position. In addition, the produced circulating loop in the middle of the tank can be effective in the mixing progress. The fluid flow pattern at the discharge region is also oriented toward the outlet pipe.

In the 22.5° layout, the tank's roof contact point is almost in the middle of the tank radius and similar to the 45° case a loop produced inside the tank. However, the loop disturbs the fluid outflow regime close to the discharge region and fluid flow pattern is not in a way that fluid goes out properly. This may be one of the reasons of the considerable difference between the mixing time of the 45° and 22.5° jet setups. In the 0° jet case, the fluid moves forward from the jet toward the discharge pipe without any internal loop. The complementary contour plots in this figure show in all setups that most regions inside the tank have low velocities, and just the fluid velocity in a narrow region close to the jet has significant values. However, according to the angle of jet the regions with higher velocities have different patterns and positions.

In this study, the effect of the size of control volumes and the employed turbulence model on the predicted fluid hydrodynamics were investigated. These variables should have significant effect on the tracer mixing prediction.

As a first step, the code was run for 60,000, 113,000, 210,000 and 600,000 number of control volumes using the RNG k–ε

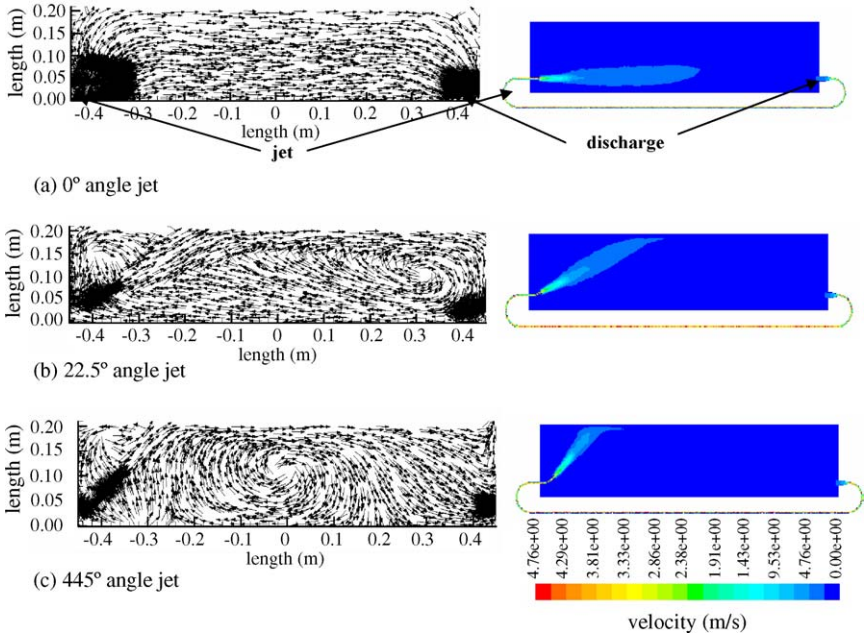

Fig. 4. The velocity flow patterns for different jet angle setups.

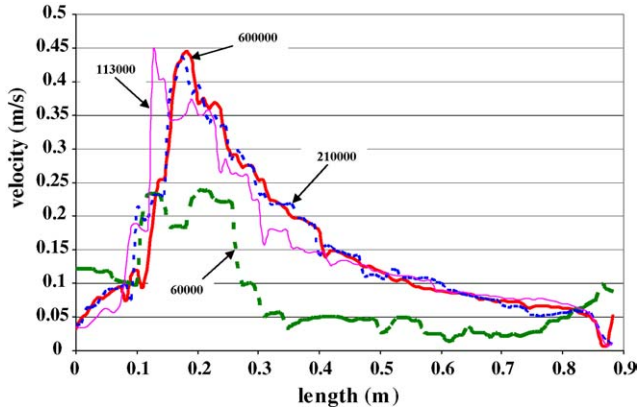

Fig. 5. The effect of number of cells on the velocity magnitudes in a line close to the tank roof for 45° jet layout.

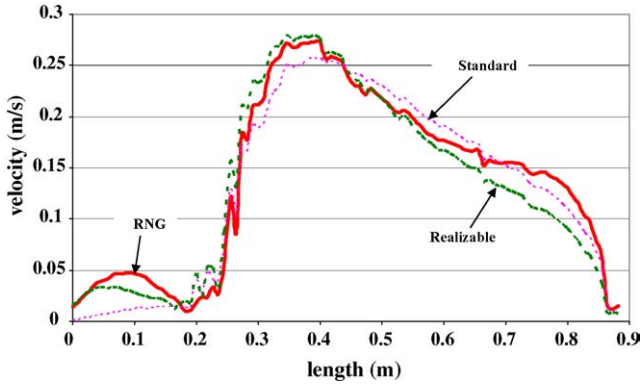

Fig. 7. The effect of the turbulence models on the velocity magnitude a line close to the tank roof for 22.5° layout.

turbulence model. Fig. 5 shows an example of the differences between the velocity predictions by these four various mesh sizes. The fluid velocity magnitudes in the 45° jet layout along an arbitrary line placed 0.5 cm below the tank roof and parallel to the jet-discharge connecting line are illustrated in this figure. The figure shows that the obtained velocity magnitudes from the 60,000 meshes have considerable difference with the others. The predicted results of the 600,000 and 210,000 layouts are quite close to each other and no significant changes are expected by using smaller mesh sizes.

The differences in fluid flow prediction have significant effect on the mixing time estimation. Fig. 6 illustrates how the mesh size can be important on the predicted mixing progress for the 45° layout using the RNG model. In this figure the mixing curves for 60,000, 113,000, 210,000 and 600,000 number of control volumes are compared with the experiment.

The figure shows that as the mesh becomes larger, the predictions error increases in a way that the 60,000 cells layout gives unsatisfactory results. On the other hand, as expected, the mixing curves of 210,000 and 600,000 setups are quite close to each other.

In the present work, the effect of using different types of turbulence model on the predicted velocity magnitudes and the mixing progress was also investigated. Fig. 7 shows the predicted velocity magnitude in the above mentioned arbitrary line for the 22.5° layout. The figure shows that the predicted velocity by the three models of turbulence have a similar trend with some differences. For example, the obtained velocities at the jet side (at the beginning of the graphs) by the standard k–ε model are lower than the RNG and realizable models predictions while at some places close to the middle of the tank the predicted values by this model are higher than others.

The effect of using different types of turbulence model on the way that the tracer spreads inside the tank is illustrated in Fig. 8 The figure shows the predicted mixing curves by the three turbulent k–ε family models using the 600,000 cells configuration.

In the 0° jet arrangement, all three theoretical curves have significant differences with the experiments in predicting the tracer spreading. However, the predicted mixing curve by the RNG model has the same trend as the experimental curve. The two other models show unexpected overshoots in the normalized tracer concentration curves.

The predicted mixing progress using the RNG model in the 22.5° arrangement is also more precise than the two other models. The predicted curve by RNG model has a peak similar to the experimental curve with a reasonable time delay, while no peak can be seen in the predicted results by the standard and realizable models. The results obtained by the standard k–ε model are quite far away from the experimental mixing curve. In addition, the predicted mixing curve by the realizable model has a significant time delay compare with the experimental curve. The best prediction results by all models were obtained in the 45° jet layout. Similar to the two other layouts, the predicting mixing curve by RNG k–ε model is closer to the experimental result and it has fluctuations similar to the experimental curve. However, the first peak in the predicted mixing curve by the standard model is much larger than the experimental one and the corresponding curves of the realizable and standard models are smoother.

The predicted 95% and 99% overall mixing times for the three jet angles using different turbulence models are shown in Table 2. The results show that the obtained mixing time is more convincing in comparison with the predicted tracer spreading

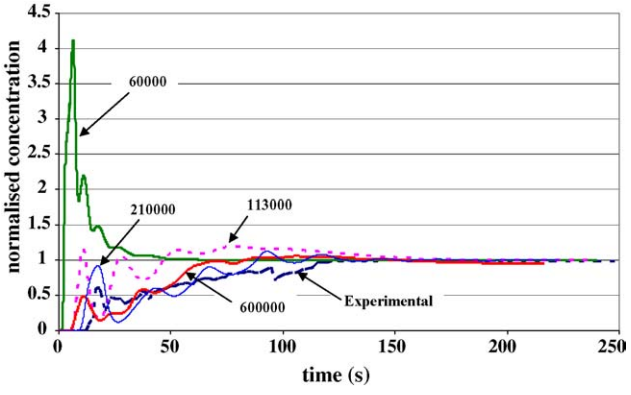

Fig. 6. The predicted mixing curves using RNG model for various numbers of control volume in 45° layout—comparison with experiment.

Table 2
The comparison between the experimental and theoretical overall mixing times

Model	0° angle jet		22.5° angle jet		45° angle jet	
	Mixing time 95% (s)	Mixing time 99% (s)	Mixing time 95% (s)	Mixing time 99% (s)	Mixing time 95% (s)	Mixing time 99% (s)
RNG	170	215	137	176	115	150
Standard	145	190	135	165	160	190
Realizable	130	200	125	175	200	245
Experiment	175	205	140	190	110	130

progress shown in Fig. 8. The results show that the obtained mixing times by the RNG k–ε model is closer to the experimental results.

It can be concluded that the size of cells and the models of turbulence can be every important in the modeling of the mixing using CFD. The results show that even small differences in the fluid flow prediction by various models of turbulence have considerable effect on the mixing prediction. The effect of number of control volumes is more important and it has significant effects on the predicted results.

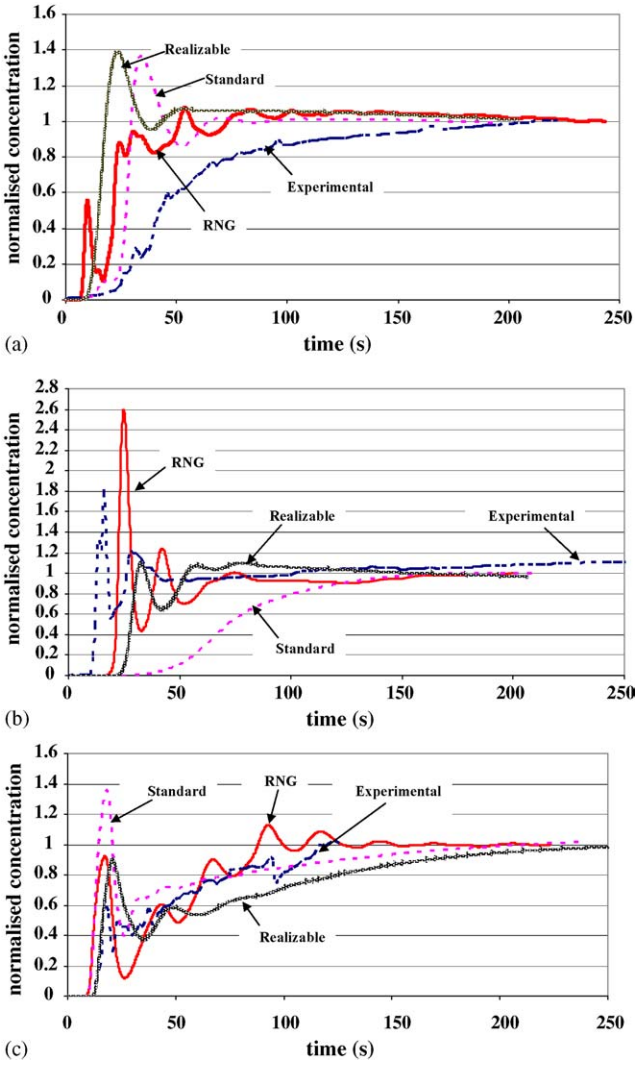

Fig. 8. The comparison between predicted and experimental mixina curves.

6. Conclusion

The CFD predicted results are convincing for predicting the mixing time. However, the predicted mixing progress can be accepted as an approximation.

- The predicted homogenization progress depends considerably on the employed model of turbulence.
- The performance of turbulence models in predicting mixing depends on the fluid flow pattern inside the tank.
- In this study, the mixing prediction using the RNG version of k–ε model gave better results in comparison with the two other models.
- The size of mesh is quite effective on the CFD prediction results.

Acknowledgment

The authors wish to express their thanks to the Kermanshah Refinery of Iran for the financial support of this work.

References

[1] H. Fossett, The action of free jets in mixing of fluids, Trans. Inst. Chem. Eng. 29 (1951) 322–332.
[2] E.A. Fox, V.E. Gex, Single-phase blending of liquids, AIChE J. 2 (1956) 539–544.
[3] A.C.G. Lane, P. Rice, An investigation of liquid jet mixing employing an inclined side entry jet, Trans. Inst. Chem. Eng. 60 (1982) 171–176.
[4] M. Yianneskis, The effect of flow rates and tracer insertion time on mixing times injet- agitated vessels, in: Proceeding of the Seventh European Conference on Mixing, Brugge, Belgium, 1991, pp. 121–128.
[5] D.R. Unger, F.J. Muzzio, R.S. Brodkey, Experimental and numerical characterization of viscous flow and mixing in an impinging jet contactor, Can. J. Chem. Eng. 76 (1998) 536–545.
[6] D.R. Unger, F.J. Muzzio, Laser-induced fluorescence technique for the quantification of mixing in impinging jets, AIChE J. 45 (1999) 2477–2486.
[7] L. Brooker, Mixing with the jet set, Chem. Eng. J. 30 (1993) 16–25.
[8] V.V. Ranade, Towards better mixing protocols by designing spatially periodic flows–the case of a jet mixer, Chem. Eng. Sci. 51 (1996) 2637–2642.
[9] S. Jayanti, Hydrodynamics of jet mixing in vessels, Chem. Eng. Sci. 56 (2001) 193–210.
[10] A.W. Patwardhan, CFD modeling of jet mixed tanks, Chem. Eng. Sci. 57 (2002) 1307–1318.
[11] H.D. Zughbi, M.A. Rakib, Mixing in a fluid jet agitated tank: effects of jet angle and elevation and number of jets, Chem. Eng. Sci. 59 (2004) 829–842.
[12] H. Feng, M. Olsen, Y. Liu, R.O. Fox, J.C. Hill, Investigation of turbulent mixing in a confined planar-jet reactor, AIChE J. 51 (2005) 2649–2663.

[13] H.K. Versteeg, W. Malalasekera, An Introduction to Computational Fluid Dynamics, The Finite Volume Method, Longman Limited, England, 1995, pp. 41–84.
[14] B.E. Launder, D.B. Spalding, Mathematical Models of Turbulence, Academic Press, England, 1974.
[15] V. Yakhot, S.A. Orszag, Renormalization group analysis of turbulence, I. Basic theory, J. Sci. Comput. 1 (1986) 1–51.
[16] T.H. Shih, W.W. Liou, A. Shabbir, J. Zhu, A new k–ε model eddy-viscosity model for high Reynolds number turbulent flows–model development and validation, Comput. Fluids 24 (3) (1995) 227–238.
[17] A.A. Alizadeh, M. Rahimi, CFD Simulation of Homogenization in Large Scale Crude Oil Storage Tanks, J. Petrol. Sci. Eng. 43 (2004) 151–161.
[18] M. Rahimi, The effect of impeller's layout on mixing time in a large scale crude oil storage tank, J. Petrol. Sci. Eng. 46 (2005) 161–170.